


RESEARCH ARTICLE

Gradual acquisition of visuospatial associative memory representations via the dorsal precuneus

Björn H. Schott^{1,2,3,4,5}  | Torsten Wüstenberg^{2,6} | Eva Lücke⁷ | Ina-Maria Pohl⁸ |
Anni Richter¹ | Constanze I. Seidenbecher^{1,5} | Stefan Pollmann^{5,8} | Jasmin M. Kizilirmak⁹ |
Alan Richardson-Klavehn³

¹Leibniz Institute for Neurobiology, Magdeburg, Germany

²Department of Psychiatry and Psychotherapy, Charité University Medicine, Berlin, Germany

³Department of Neurology, Otto von Guericke University Magdeburg, Magdeburg, Germany

⁴Department of Psychiatry and Psychotherapy, University Medicine Göttingen, Göttingen, Germany

⁵Center for Behavioral Brain Sciences (CBBS), Magdeburg, Germany

⁶Systems Neuroscience in Psychiatry (SNiP), Central Institute of Mental Health, Mannheim, Germany

⁷Department of Pulmonary Medicine, Otto von Guericke University Magdeburg, Magdeburg, Germany

⁸Institute of Psychology, Otto von Guericke University Magdeburg, Magdeburg, Germany

⁹Institute of Psychology, University of Hildesheim, Hildesheim, Germany

Correspondence

Björn Hendrik Schott, Leibniz Institute for Neurobiology, Brenneckestr. 6, 39118 Magdeburg, Germany.
Email: bschott@lin-magdeburg.de

Funding information

Leibniz-Gemeinschaft; Deutsche Forschungsgemeinschaft, Grant/Award Numbers: SFB 779, TP A04; SFB 779, TP A08; SFB 779, TP A10; SFB 779, TP B14

Abstract

Activation of parietal cortex structures like the precuneus is commonly observed during explicit memory retrieval, but the role of parietal cortices in encoding has only recently been appreciated and is still poorly understood. Considering the importance of the precuneus in human visual attention and imagery, we aimed to assess a potential role for the precuneus in the encoding of visuospatial representations into long-term memory. We therefore investigated the acquisition of constant versus repeatedly shuffled configurations of icons on background images over five subsequent days in 32 young, healthy volunteers. Functional magnetic resonance imaging was conducted on Days 1, 2, and 5, and persistent memory traces were assessed by a delayed memory test after another 5 days. Constant compared to shuffled configurations were associated with significant improvement of position recognition from Day 1 to 5 and better delayed memory performance. Bilateral dorsal precuneus activations separated constant from shuffled configurations from Day 2 onward, and coactivation of the precuneus and hippocampus dissociated recognized and forgotten configurations, irrespective of condition. Furthermore, learning of constant configurations elicited increased functional coupling of the precuneus with dorsal and ventral visual stream structures. Our results identify the precuneus as a key brain structure in the acquisition of detailed visuospatial information by orchestrating a parieto-occipito-temporal network.

KEYWORDS

fMRI, hippocampus, long-term memory, precuneus, visuospatial memory

1 | INTRODUCTION

The hippocampus and adjacent medial temporal lobe (MTL) regions have long been recognized as key brain structures that mediate the encoding of novel information into explicit long-term memory (Düzel, Bunzeck, Guitart-Masip, & Düzel, 2010; Ranganath & Rainer, 2003). The MTL memory system does, however, not operate in isolation, and human neuroimaging studies have convergently shown that both

encoding and retrieval of explicit memory traces almost invariably engage the hippocampal memory network in conjunction with neocortical, particularly prefrontal and parietal, structures (Rugg, Otten, & Henson, 2002; Wagner, Shannon, Kahn, & Buckner, 2005).

Parietal cortical activations have been frequently observed in functional neuroimaging studies of explicit, and particularly context-rich episodic, retrieval (Ciaramelli, Grady, & Moscovitch, 2008; Hutchinson, Uncapher, & Wagner, 2009; Sestieri, Shulman, & Corbetta, 2017), and a

dorsal–ventral distinction of retrieval-related attentional processes has been proposed in the attention-to-memory (AtoM) model (Ciaramelli et al., 2008). The AtoM model focuses on lateral parietal structures, but episodic retrieval also engages medial parietal cortices like the ventral precuneus and adjacent posterior cingulate cortex (PCC). Together with ventral and posterior parts of the temporoparietal junction (TPJ), particularly the angular gyrus (ANG), these structures are considered to form core regions of the default mode network (DMN; Buckner, Andrews-Hanna, & Schacter, 2008), but Gilmore et al. further suggested the presence of a parietal memory network (PMN) that, despite its close proximity to the posterior DMN, could be distinguished from the latter (Gilmore, Nelson, & McDermott, 2015). The PMN as proposed by Gilmore et al. is functionally characterized by showing increased neural responses to repeated relative to novel stimuli, a pattern that has been referred to as repetition enhancement (RE; Segaert, Weber, de Lange, Petersson, & Hagoort, 2013).

Despite the prominent involvement of parietal structures in memory retrieval, the role of the parietal cortex in the *encoding* of information into long-term memory is less well understood. Notably, ventral parietal structures and particularly the PMN, have been shown to exhibit negative subsequent memory effects during encoding of novel information, that is, higher activity in these regions has been associated with subsequent forgetting rather than remembering (Gilmore et al., 2015; Kim, 2011; Uncapher & Wagner, 2009). On the other hand, positive subsequent memory effects in parietal cortices have also been observed, and they have commonly been found in more dorsal parietal regions like the dorsal precuneus, the superior parietal lobule (SPL) and the adjacent intraparietal sulcus (Uncapher & Wagner, 2009). These structures are well-known for their key role in visual cognition, including spatial attention and working memory (Cabeza et al., 2003, 2008; Corbetta, Kincade, & Shulman, 2002; Pollmann & von Cramon, 2000), distractor suppression (Pollmann et al., 2003) or visual imagery (Byrne, Becker, & Burgess, 2007; Handy et al., 2004). In an attempt to integrate those observations with the response pattern of the more ventral PMN, that is, negative subsequent memory effects, followed by RE (*encoding–retrieval flip*; Gilmore et al., 2015), one might consider the possibility of dissociable roles for dorsal as compared to ventral parietal structures within a more extended parietal lobe memory system. One such possible distinction could be a preferential activation of dorsal parietal structures during encoding of spatial information, as observed in a study of attentional modulation of encoding (Uncapher & Rugg, 2009). In line with a prominent role of parietal structures in spatial memory formation, precuneus activity has been associated with memory performance during spatial navigation (Brodt et al., 2016). However, the overall evidence as to whether this actually reflects a specialization is yet inconclusive (Uncapher & Wagner, 2009).

In the light of both the prevailing pattern of parietal RE (Gilmore et al., 2015) and the repeatedly observed positive subsequent memory effects in dorsal parietal regions implicated in visuospatial cognition (Uncapher & Rugg, 2009; Uncapher & Wagner, 2009), we aimed to address the possibility that parietal cortical structures like the precuneus might support the acquisition of complex visuospatial information during repeated exposure. To this end, we investigated the encoding of icon–location associations on distinctive backgrounds over five consecutive

days, conducting functional MRI on Days 1, 2, and 5 (Figure 1). Half of the configurations were kept constant across the days, while the other half were reshuffled for each day. Successful encoding was probed after each learning session, and the formation of persistent memory traces was tested in a short delayed memory test after another 5 days. At the behavioral level, we hypothesized that constant, but not shuffled, configurations would be associated with significant learning improvement over 5 days and with better memory performance in the delayed test. At the level of brain activity, we hypothesized that during the acquisition of constant configurations, parietal cortices like the precuneus would be increasingly involved (Gilmore et al., 2015; Kafkas & Montaldi, 2014), whereas the hippocampus would display decreasing involvement over time (Brodt et al., 2016), as the constant configurations become increasingly familiar (Nyberg, 2005). Considering the previously reported specific activation of the dorsal precuneus in attentionally modulated encoding of spatial information (Uncapher & Rugg, 2009), we further explored the possibility that RE for constant configurations might be more pronounced in the dorsal compared to the ventral precuneus. To assess the importance of parietal activations for the actual *encoding* of the configuration, we additionally tested, whether the precuneus or adjacent parietal structures might also predict successful memory formation, as assessed with a subsequent memory contrast and with a correlation of precuneus activity with delayed memory performance. Finally, we conducted a functional connectivity analysis, guided by the assumption that, during spatial memory formation, the precuneus would most likely not act in isolation, but rather exhibit memory-related functional connectivity with brain structures more directly involved in visuospatial information processing.

2 | METHODS

2.1 | Participants

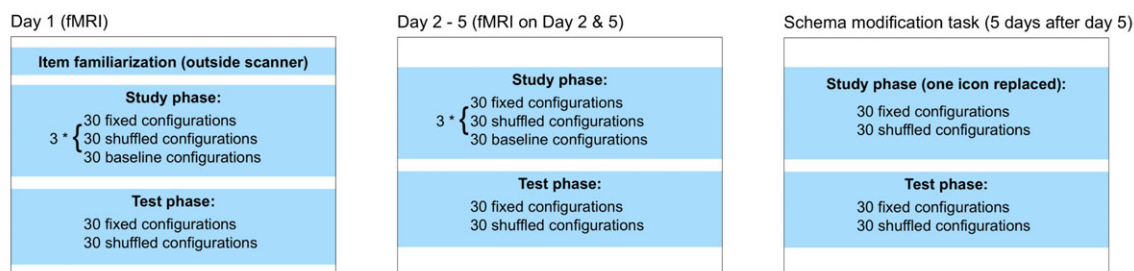
A total of 34 participants were recruited for the study. The data sets from two participants had to be excluded from data analysis due to technical difficulties resulting in incomplete recording of behavioral or functional magnetic resonance imaging (fMRI) data. The remaining 32 participants (12 women and 20 men) had an age range between 19 and 34 years (mean age = 25.3 years, $SD = 3.5$ years). All participants were right-handed and native speakers of German according to self-report, reported no history of neurological or psychiatric illness, were free of MRI contraindications, and had normal or corrected-to-normal vision. Participants gave written informed consent to participate in the study in accordance with the Declaration of Helsinki (World Medical Association, 2013), and the study was approved by the Ethics Committee of the University of Magdeburg, Faculty of Medicine.

2.2 | Task design and behavioral paradigm

2.2.1 | Overview

The study was designed as a longitudinal within-subjects investigation. Participants performed an object–location learning task (positions of icons in front of a background picture) with study and test sessions on each of five consecutive days (Figure 1a). On each of these 5 days,

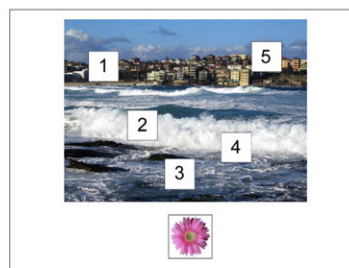
(a) Overview



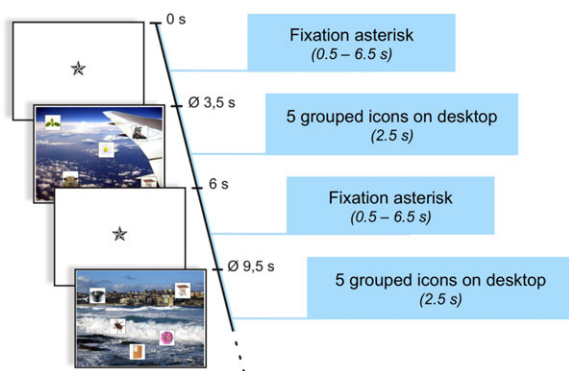
(b) Example study stimulus



(c) Example test stimulus



(d) Example study trial



(e) Example test trial

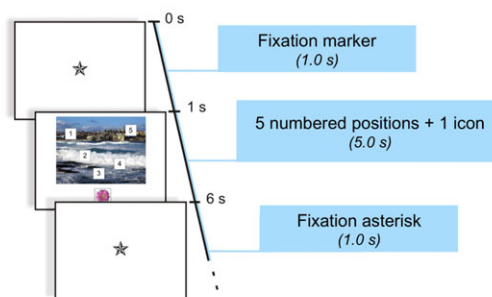


FIGURE 1 Experimental paradigm. (a) Overview. (b) Example stimulus from the study phase. (c) Example stimulus from the test phase. (d) Trial sequence of the study phase. (e) Trial sequence of the test phase

participants studied 30 constant and 30 changing (shuffled) configurations, as well as 15 repetitions of each of 2 highly familiar configurations that served as baseline configurations over three runs, followed by a location retrieval task 30 min after the third study run. Consequently, in the constant condition, each of the configurations had been presented $5 \times 3 = 15$ times at the end of Day 5, whereas in the shuffled condition, the number of presentations per configuration was always three (i.e., the three presentations on each of the 5 days, which were constant only within a day). Therefore, although short-term spatial learning of shuffled configurations was also possible (i.e., within a day), only constant configurations could plausibly result in the formation of long-term memory representations across the 5 days. The baseline trials consisted of a constant background image that was presented with two alternating configurations of five icons not used in the experimental conditions of interest. The specific icons and background images were randomly assigned to the conditions across participants. Five days after the last learning day, the delayed memory task was performed as a single study-test cycle. During study, the constant and shuffled configurations learned previously were presented, with the icon probed in the test phase of Day 5 being

substituted with another icon from the participant's individual set (see Section 2.2.2). In the following retrieval test, the positions of the substituted icons were probed, using the same setup as in the retrieval tests of the main experiment. We hypothesized that participants would form more stable memory representations in the constant condition, such that, even after the substitution of one icon, retrieval accuracy would be higher for icons from previously constant compared to shuffled configuration.

2.2.2 | Stimulus material

Each study stimulus consisted of five icons (natural and man-made objects on a white square-shaped background) that were pseudorandomly placed in front of a background picture (photographs of outdoor scenes). Background images were obtained from the Corel Stock Photo Library, which has previously been employed in a study of visual scene processing (Rieger et al., 2013). A total of 90 outdoor scenes were selected from the library by author E.L. and visually inspected to ensure that no human beings were depicted in the pictures. All images were resized to a resolution of 800×600 pixels. Sixty of these images were selected for each participant to reduce

item effects across the group and pseudorandomly assigned to the conditions (constant and shuffled). Icons consisted of square images depicting color photographs of artificial ($N = 90$) or natural ($N = 50$) objects in front of a white background. The icons were selected from stimulus sets assembled for previously published studies (Barman et al., 2015; Handy et al., 2004; Herbort et al., 2016) and resized to 100×100 pixels. Thirty icons per category were selected for each participant and pseudorandomly assigned to the trials, resulting in each icon being presented in three to seven different trials. The purpose of repeating icons across trials was to ensure that participants actually studied the icon positions in their specific context (i.e., in relation to the background image and the other icons) rather than relying on item uniqueness. Variability of frequency (3–7) was introduced to avoid implicit learning of icon frequencies across trials, thereby reducing expectancy effects. In baseline trials, one single background image with two alternating sets of icons was used for all participants, and none of those images were used in the conditions of interest. Figure 1b depicts an example stimulus from the study phase. Stimuli of the test phase consisted of the background images from the study phase, with the positions marked with numbers from 1 to 5, and one of the original icons displayed below (Figure 1c).

2.2.3 | Paradigm (main experiment)

Before entering the MRI scanner on Day 1, participants were familiarized with the stimulus material. In the first part of the familiarization phase, all subsequently used background images were presented sequentially for 3 s each, in order to reduce item novelty during the actual task.¹ The two baseline configurations (i.e., the baseline background image with the two fixed sets of icons) were presented alternately with the background images. Both baseline configurations were thus presented 30 times during familiarization, allowing participants to learn them to ceiling already before the start of the actual experiment. In the second part of the familiarization phase, all icons were presented for 3 s each. Participants were instructed to carefully attend to the depicted images, as these would be important in the upcoming experiment. After the familiarization, participants received a written instruction describing the task and were given the opportunity to ask the experimenter for further explanations.

Behavioral pilot data from 10 young, healthy volunteers had shown that the strongest increase in correct response rates in the constant condition occurred from Day 1 to 2, followed by a further, slower, performance increase between Days 2 and 5 (unpublished observations by authors E.L. and B.S.). Therefore, the study phase of the actual experiment was performed inside the MRI scanner on Days 1, 2, and 5, and outside the scanner on Days 3 and 4. Each trial of the study phase consisted of five icons positioned on a background image (hence referred to as spatial configuration). Participants were instructed to respond via button press (right index or middle finger) whether more icons depicted natural (or “living”) or artificial

(“nonliving”) objects. The purpose of this task was to ensure that participants actually attended to the study items. They were also instructed to try and explicitly memorize the positions of the icons on the background pictures. Each spatial configuration was presented for 2.5 s and followed by a variable fixation delay. The duration of the delay was jittered between 0.5 and 6.5 s, using a near-exponential distribution to improve the estimation of the trial-specific hemodynamic response function (HRF) for each condition (Hinrichs et al., 2000). Each study phase consisted of three runs of 90 trials each. Thirty trials comprised configurations that were kept constant over the 5 days of the experiment (*constant configurations*), and 30 trials contained configurations in which the positions of the icons were redistributed across days, using a Latin square design, such that no icon was displayed twice in the same position (*shuffled configurations*). The purpose of the high number of configurations (30 per condition) was to ensure that learning of the configurations would occur gradually over time and to avoid ceiling effects during early phases of the experiment. The remaining 30 trials of each run were 15 presentations of each of two baseline configurations, in which the same background image was presented repeatedly along with either three natural and two artificial icons or vice versa, with the two sets of icons and their respective positions kept constant throughout the experiment. We used two different baseline configurations to ensure that participants performed the study task also with the baseline trials. During data analysis (see below), the baseline trials served as a high-level control condition with comparable visual and motor stimulation but little further learning due to the likely ceiling effect from the presentation during the familiarization phase. Figure 1d depicts the detailed timing of the study phase.

The test phase was performed on a desktop computer 30 min after the end of the study phase. The background pictures from the study phase (constant and shuffled configurations, but not baseline configurations) were presented with the numbers from 1 to 5 in the positions of the icons from the study phase and a single icon in a central position below the background picture. Participants were requested to recall the position of the icon presented below and indicate the position via key press. To reduce guessing, participants were further asked to press the space bar key when they could not remember the position of the depicted icon. Test stimuli were presented for 5 s, followed by a fixation delay of 1 s. As in the study phase, instructions were given in written format, followed by the opportunity to ask questions for further clarification. The detailed trial timing of the test phase is depicted in Figure 1e.

2.2.4 | Paradigm of the delayed memory task

Five days after the last learning day, an additional single study-test cycle was performed. The study phase consisted of a single run in which 60 items were presented as in the main experiment (30 constant and 30 shuffled configurations, omitting the baseline configurations). In each configuration, the icon probed in the test phase of the last learning day was replaced with a new icon in the same position. These substituted icons were probed in the test phase of the delayed memory test, using the same instructions as in the main learning task.

¹Due to a randomization error, the background images of the constant condition ($N = 30$) were always presented before the background images of the shuffled condition ($N = 30$). While no clear primacy or recency effect could be observed in subsequent analyses, there was an unexpected difference in behavioral performance between the two conditions on Day 1. For details, please refer to the results, discussion, and figures (Supporting Information).

2.3 | MRI data acquisition

Structural and functional brain images were acquired on a 3T Siemens MAGNETOM Trio MRI scanner (Siemens, Erlangen, Germany) equipped with an eight-channel phased-array head coil. In each functional run, 270 whole-brain T2*-weighted echo-planar images (EPIs) were acquired (TR = 2.0 s, TE = 30 ms, flip angle = 80°, 33 axial slices, ascending odd-even interleaved acquisition order, in-plane resolution = 64 × 64 voxels, voxel size = 3.5 × 3.5 × 3.5 mm). On one of the scanning days, a high-resolution T1-weighted 3D magnetization-prepared rapidly acquired gradient-echo (MPRAGE) image with an isotropic resolution of 1 mm³ was acquired to improve spatial normalization, and for display purposes (see below).²

2.4 | Data processing and analysis

Data processing and analysis of fMRI data was performed using *Statistical Parametric Mapping* (SPM12, Wellcome Trust Centre for Neuroimaging, University College London, London, UK).

2.4.1 | Preprocessing

Images were corrected for acquisition delay and head motion, using the algorithms implemented in SPM12. To optimize transformation into stereotactic reference space, the T1-weighted MPRAGE image was then coregistered to the mean EPI obtained from motion correction, segmented into tissue classes and warped to the brain template provided by the International Consortium for Brain Mapping (ICBM) using the segmentation algorithm provided by SPM. EPIs were normalized into the ICBM stereotactic reference frame using the normalization parameters obtained from segmentation (final voxel size = 3 × 3 × 3 mm³). Normalized EPIs were smoothed with a Gaussian kernel of 8 mm³ full width at half maximum. Finally, to remove low-frequency noise, a 1/128 Hz temporal high-pass filter was applied to the data.

2.4.2 | Statistical analysis of fMRI data

Statistical analysis was performed using a two-stage mixed-effects model. At the first stage, learning-related blood-oxygen-level-dependent (BOLD) responses were analyzed as a function of trial category (constant vs. shuffled) and learning day (1, 2, or 5), using the general linear model (GLM) approach of SPM12. Regressors for each stimulus category were created by modeling the mean brain responses to constant, shuffled, and baseline configurations, separated by run. Thus, the model contained nine runs (three per day) consisting of three regressors representing the learning-associated brain responses. Signal fluctuations caused by head motion were modeled by means of the six rigid-body movement parameters determined from motion correction.³ Finally, a constant regressor represented the implicit baseline of the time course (i.e., the mean over scans). Model estimation was performed using a restricted maximum likelihood fit as implemented

in SPM12. The *t* contrasts comparing constant and shuffled trials to baseline trials were computed separately for each day (Day 1: Runs 1–3, Day 2: Runs 4–6, Day 5: Runs 7–9) in the first-level models of all participants and submitted to second-level random-effects analyses. At the second stage of the model, the resulting single subjects' contrast images were then submitted to second-level random effects analyses. Comparisons of constant and shuffled configurations were based on a full-factorial ANOVA model with category (constant vs. shuffled) and day (three levels for Days 1, 2, and 5) as factors, and between-subject variance in global signal was modeled by N-1 subject covariates. The significance level was set to $p < .05$, family-wise error (FWE) corrected at cluster level with an a priori statistical search threshold of $p < .001$, uncorrected, as previously recommended for cluster-based corrections (Eklund, Nichols, & Knutsson, 2016; Woo, Krishnan, & Wager, 2014). To obtain a single contrast value reflecting the study of constant versus shuffled configurations for the definition of a cluster employed for time course extraction in the functional connectivity analysis and for exploratory brain-behavior correlations, we computed first-level *t* contrasts testing brain responses to constant versus shuffled spatial configurations on Days 2 and 5. Those were submitted to a one-sample *t* contrast at second level (inclusively masked with the condition by day interaction *F* contrast).

A separate ANOVA model was generated to assess neural correlates of successful versus unsuccessful encoding of the stimuli (DM effect; difference due to memory; Paller, Kutas, & Mayes, 1987). To this end, we computed an additional set of first-level GLMs, in which constant and shuffled configurations were further divided into later remembered and later forgotten configurations. A second-level full-factorial ANOVA model (condition by day) was then computed on the first-level *t* contrasts testing remembered against forgotten trials for each condition and day.⁴ Based on our a priori hypotheses regarding the hippocampus and the precuneus, we computed region of interest (ROI) analyses in both structures. Given the previous literature regarding the role of the medial prefrontal cortex (mPFC) in memory formation based on prior representations (van Kesteren, Ruiters, Fernandez, & Henson, 2012), we also performed ROI analyses in the mPFC. Furthermore, an exploratory voxel-wise whole-brain analysis was performed at $p < .001$, uncorrected, with a minimum cluster size of 10 voxels, to assess the specificity of encoding-related activations in the hippocampus and precuneus.

All ROIs were defined on the basis of anatomical constraints and previous publications, independently of our current results, thus avoiding circularity (Kriegeskorte et al., 2010; see below for details on ROI generation). The significance level in the ROI analyses was set to $p < .05$, FWE corrected for the respective ROI volumes at voxel level, with an a priori search threshold of $p < .001$, uncorrected. For visualization purposes, activations were superimposed onto the group mean of the participants' individual T1-weighted MR images using the MRIcron⁵ software package.

²In four participants, MPRAGE images with 1 mm³ voxel size were not available, and the MPRAGE images with 2 mm³ voxel size acquired for slice positioning were used for normalization instead.

³Analysis of the movement parameters as a function of day and run is provided as supplementary online material.

⁴The subsequent memory analysis was conducted in 31 of the 32 participants, because one participant had no correct responses in the shuffled condition on Day 1. All other participants had at least two trials in all conditions.

⁵<http://people.cas.sc.edu/rorden/micron/index.html>

2.4.3 | Regions of interest

ROIs were defined based on anatomical and literature-based functional constraints. ROIs of the left and right hippocampus were defined based on the SPM Anatomy Toolbox (Eickhoff et al., 2005) and included the dentate gyrus, CA regions, and the subiculum. Dorsal and ventral precuneus ROIs and an additional mPFC ROI were defined using a combined anatomical and probabilistic approach as described previously (Schott et al., 2013; Schubert et al., 2008). Coordinates were obtained from previous fMRI studies finding precuneus activations during memory tasks (for details see Methods, Supporting Information). The distributions of thus obtained coordinates were fit as three-dimensional Gaussian ellipsoids, limited to voxels within the 2 SD borders of these Gaussian models. Due to overlapping ellipsoids for ventral and dorsal coordinate sets, the final ROIs (or, more precisely, the border between precuneus subregions) were computed by means of a maximum probability approach. Finally, we inclusively masked the resulting ROIs with anatomical boundaries obtained from the Automated Anatomical Labeling Atlas (Tzourio-Mazoyer et al., 2002). Complete lists of coordinates and representative sections of the ROIs are provided as Supporting Information, and the MATLAB toolbox used for ROI generation as well as the SPM images of the ROIs are available from the authors upon request.

2.4.4 | Functional connectivity analysis

In order to elucidate the network by which, according to our results, the precuneus mediates learning of complex visuospatial associative information and, specifically, to assess whether this network encompasses—or bypasses—the hippocampus, we employed the psychophysiological interaction (PPI) approach (Friston et al., 1997). PPI analysis captures the modulation of functional connectivity between brain structures as a function of an experimental or psychological context (Friston et al., 1997; Gitelman, Penny, Ashburner, & Friston, 2003). Based on the results of our GLM-based analysis, which suggests a key role for the precuneus in the network involved in visuospatial long-term memory formation (see Section 3), we chose this structure as the seed region. At the single-subject level, GLM-based PPI models were computed. Volumes of interest were defined as spheres ($r = 6$ mm). To obtain a balanced trade-off between anatomical specificity and adequate signal-to-noise ratio, the precuneus activation cluster from the t contrast constant against shuffled spatial configurations served as a spatial constraint. Within this cluster, spheres were centered on the local maxima of the *effects of interest* contrast⁶ individually for each subject (for detailed description of a similar approach, see Soch et al., 2017). For each participant, the first eigenvariate time series were extracted from these spheres and deconvolved with the canonical HRF (Friston et al., 1997; Gitelman et al., 2003). This combined anatomical and functional definition of the seed regions was chosen to achieve a reasonable tradeoff between anatomical specificity and signal-to-noise ratio. The resulting time series were convolved with the psychological function P, which was defined as congruency (constant minus shuffled configurations) and subsequently reconvolved with the HRF, yielding the new

variable X, which was entered as primary covariate of interest into a new first-level GLM. The original BOLD eigenvariate time series and the psychological variable P convolved with the HRF formed further covariates in the GLM design matrices. We also included the regressors of the baseline stimuli and the six movement parameters determined as covariates of no interest, plus a constant representing the mean over scans. At second level, a one-way within-subjects ANOVA with the three-level factor day (1, 2, and 5)⁷ was computed, using regressors of no interest to covary for subject-related variance as described above. As in the main GLM analysis, the significance level was set to $p < .05$, FWE corrected at cluster level with an a priori statistical threshold of $p < .001$. Because of our a priori hypothesis that the hippocampus would be part of the precuneus-centered spatial learning network, we also performed ROI analyses in the left and right hippocampus, using ROIs generated with the SPM Anatomy Toolbox (Eickhoff et al., 2005). The significance level was set to $p < .05$, FWE corrected for the ROI volumes at voxel level.

2.4.5 | Behavioral data analysis

Analysis of participants' responses during the test phase was performed using MATLAB R2014b (MathWorks, Natick, MA) and SPSS 22.0 (IBM, Armonk, NY). Proportions of correct responses, incorrect responses, and "don't know" or omitted responses (grouped together as *omissions*) were submitted to separate two-way ANOVAs for repeated measures, with each ANOVA including the factors *condition* (constant vs. shuffled configurations) and *day* (1, 2, 3, 4, and 5). To account for sphericity violations, degrees of freedom were corrected using the Greenhouse–Geisser correction when applicable. Paired t tests were computed to assess condition-specific effects underlying the interactions revealed by the ANOVAs. Paired t tests were also employed to assess expected differences between recognition rates of constant versus shuffled configurations in the test phase of the delayed memory test. Effect sizes (Cohen's d) were computed as described by Morris and DeShon (2002). To test for robustness of the expected performance differences on each day of study as well as in the delayed memory test, the 95% confidence intervals of the differences (constant and shuffled) were estimated via bootstrap resampling (Efron & Tibshirani, 1993), using the percentile- t method (10,000 iterations for confidence interval estimation and 200 iterations for variance estimation).

2.4.6 | Brain-behavior correlations

In order to assess a suspected relationship between BOLD responses to the repeated exposure to spatial detail (i.e., icon positions in the constant vs. shuffled condition) and the long-term encoding success, brain-behavior correlations were performed. To this end, we first computed the single subjects' t -contrasts testing constant against shuffled configurations on Days 2 and 5, thereby obtaining a single value representing the learning-related brain response in each subject. The resulting contrast images were submitted to a one-sample t -test model at group level, and the first eigenvariate was extracted from the peak voxel of the resulting cluster in the precuneus. Using this

⁶The effects of interest contrast, described by an eye matrix over all covariates of interest, capture overall variance explanation in an unbiased manner.

⁷The factor *condition* from the ANOVA model of the main GLM analysis was coded differentially in the psychological and interaction variables.

TABLE 1 Recognition performance for constant and shuffled configurations

Day	Constant		Shuffled		t_{31}	p	Cohen's d
	Mean	SD	Mean	SD			
1	.288	.122	.201	.082	3.99	<.001	.724
2	.431	.135	.252	.103	6.84	<.0001	1.213
3	.484	.133	.291	.092	6.83	<.0001	1.157
4	.514	.141	.318	.102	8.67	<.0001	1.572
5	.533	.160	.294	.122	10.61	<.0001	1.922
Delayed memory	.274	.130	.217	.092	2.36	.025	.419

Proportions of correctly recognized icon positions are shown, separated by condition (constant vs. shuffled). SD = standard deviation. All t and p values are from paired t tests comparing recognition rates of constant versus shuffled configurations on each learning day.

approach, the brain activity measure was obtained independently of the behavioral data, thereby avoiding circularity (Kriegeskorte et al., 2010). The behavioral measure of interest was the difference of proportions of correct responses between the constant and shuffled conditions in the delayed memory test. We first performed Spearman's rank correlations, followed by outlier-robust Shepherd's P_i correlations (Schwarzkopf et al., 2012). Shepherd's P_i correlations have been proposed as a method to improve robustness of brain-behavior correlations, which have been criticized for their susceptibility to outliers (Rousselet and Pernet, 2012; Schwarzkopf et al., 2012). The approach is based on Spearman's correlation and additionally includes a bootstrap-based estimation of the Mahalanobis distance, thereby allowing for an unbiased detection and exclusion of outliers.

3 | RESULTS

3.1 | Behavioral results

Table 1 displays the participants' recognition rates (proportions of correctly recognized positions) during the test phases, separated by condition (constant vs. shuffled) and day. Detailed response data are shown in Table S5, Supporting Information. Statistical analysis of recognition accuracy revealed an increase of memory performance for the icon positions in the constant condition over the experimental sessions (Days 1–5), with the most pronounced increase from Day 1 to 2 (Figure 2; Table 1). A two-way ANOVA for repeated measures revealed main effects of both condition (constant vs. shuffled; $F_{1,31} = 151.89$, $p < .001$ partial $\eta^2 = .830$) and day ($F_{2,5,79,0} = 31.36$, $p < .001$, partial $\eta^2 = .503$) as well as a significant condition by day interaction ($F_{3,6,113,0} = 6.61$, $p < .001$, partial $\eta^2 = .176$). A paired t test comparing the learning rates between the conditions (proportions of correct responses on Day 5–1) yielded a significantly higher learning rate in the constant condition ($t_{31} = 5.11$, $p < .001$, Cohen's $d = .913$). Paired t tests with effect size calculation (Cohen's d) further showed that the differences between the recognition rates of the two conditions increased from Day 1 to 5 (Table 1). Please see also Results and Discussion (Supporting Information) for further details regarding the response patterns to constant and shuffled configurations.

In the test phase of the delayed memory task 5 days later, constant spatial configurations were associated with a significantly higher proportion of correctly recognized icon positions when compared to shuffled spatial configurations ($t_{31} = 2.36$, $p = .025$, two-tailed; see

Figure 2, right), suggesting that constant configurations were still associated with better memory performance after 5 days (see Table 1 for details).

3.2 | Functional MRI results

3.2.1 | Condition-independent neural repetition effects

We first assessed BOLD signal increases and decreases as a function of repeated stimulus presentation across the two conditions (constant and shuffled), in order to evaluate unspecific item-related repetition effects that were independent of the precise icon positions. A two-way ANOVA (condition by day) revealed a main effect of day, pointing to configuration-type independent novelty and familiarity responses. The *novelty* (or repetition suppression, RS) contrast (contrasting activity on Day 1 against the mean activity on Days 2 and 5; Day 1 > [Day 2 + Day 5]/2) revealed that the familiarization-related brain response decreased in an occipitotemporal cluster encompassing portions of the cuneus and ventral precuneus. In an ROI-based analysis, a condition-independent novelty response was also found in the left hippocampus ($[x, y, z] = [-33, -22, -13]$, $t_{155} = 3.51$, $p = .032$, FWE corrected for ROI volume at voxel level). Furthermore, novelty responses were observed in the ventral striatum and in the bilateral TPJ (Table 2). On the other hand, the inverse contrast (*familiarity*: Day 1 < [Day 2 + Day 5]/2) revealed pronounced familiarity (or RE) responses in a distributed network, with strongest RE observed in a portion of the right precuneus that extended into the retrosplenial cortex. RE could also be found in lateral parietal, inferior temporal (fusiform and parahippocampal) and lateral prefrontal cortices (Table 3).

3.2.2 | Condition-dependent brain activity patterns (constant vs. shuffled)

To assess the neural processes specifically associated with the learning of constant compared to shuffled configurations, we compared brain responses to constant and shuffled learning stimuli on Days 2 and 5 (inclusively masked with the condition by day interaction F contrast, thresholded at $p < .05$ uncorrected). In the thus masked contrast, we observed pronounced activation in a superior medial parietal brain region, which was the only activation cluster that survived a cluster-based FWE correction. Using the SPM Anatomy Toolbox (Eickhoff et al., 2005), this region was identified as belonging to the precuneus; Figure 3a displays activation in the

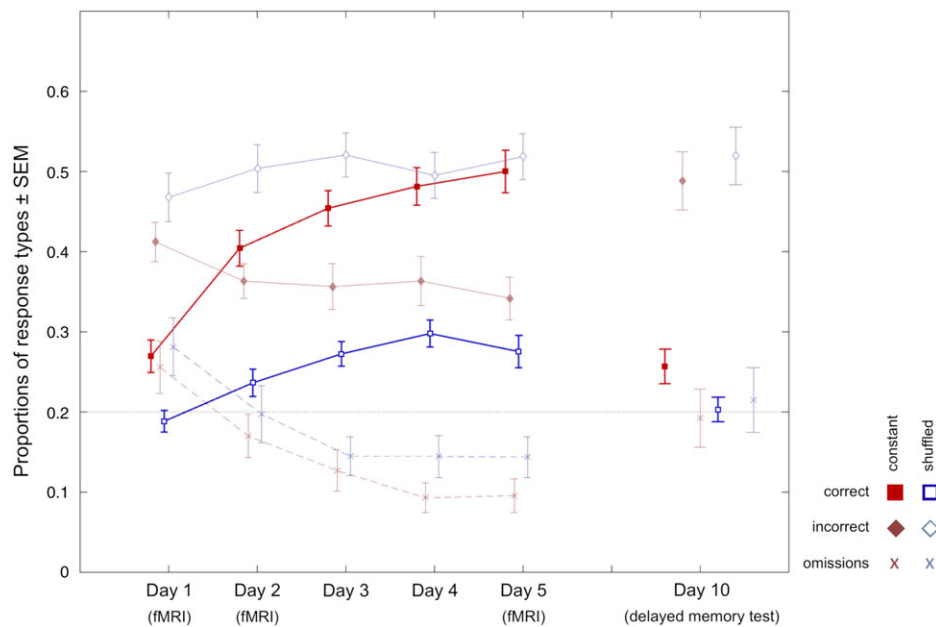


FIGURE 2 Behavioral results. Learning curves display proportions of correct, incorrect, and omitted responses in the test phase from Day 1 to 5, separately for constant (red) and shuffled (blue) configurations. Plots on the right display responses 5 days after the last learning day. Error bars depict 95% confidence intervals as estimated via bootstrap resampling

dorsal precuneus as a function of condition and day. To further localize the activation cluster within the precuneus, we assessed its relative extent in four precuneus ROIs (dorsal vs. ventral \times left vs. right). Among the voxels in the precuneus that showed a significant subsequent memory effect at $p < .001$, uncorrected, 88% were located in the dorsal precuneus, predominantly in the right hemisphere (Figure 3b). In an exploratory analysis, we omitted the masking with the interaction contrast, revealing a further activation cluster in inferior occipital cortex that extended from early visual areas to portions of the ventral visual stream (Table 4). The reverse contrast (shuffled $>$ constant configurations on Days 2 and 5) revealed no activations that remained significant after correction at either voxel or cluster level.

TABLE 2 Novelty-related brain responses: Day 1 $>$ (Day 2 + Day 5)

Cluster size	p_{FWE} (cluster)	Brain structure	x, y, z (mm)	SPM{T}
385	<.001	Right cuneus/precuneus	9, -82, 32	7.24
		Left cuneus	-3, -82, 26	6.72
176	.003	Right ventral striatum	15, 5, -7	4.74
		Right amygdala	21, 2, -13	4.45
89	.041	Left amygdala	-21, -4, -10	4.18
		Left superior temporal gyrus	-45, -34, 17	4.00
83	.050	Right supramarginal gyrus	-60, -34, 20	3.84
		Right rolandic operculum	54, -28, 26	4.24
			63, -25, 26	3.77
			60, -19, 17	3.42

FWE = family-wise error; FWEc = family-wise error correction; SPM = Statistical Parametric Mapping.

SPM{T} contrast results are displayed at $p < .05$, FWE corrected at cluster level with an a priori search threshold of $p < .001$. Minimum cluster size for (FWEc) = 83 voxels. Coordinates are given in MNI space.

3.2.3 | Neural correlates of successful encoding—DM effect

A comparison of brain responses to subsequently recognized configurations compared with those which were not recognized (false responses and omissions) revealed that both the hippocampus and the right dorsal precuneus exhibited more pronounced activation during study of

TABLE 3 Familiarity-related response increases across days (Days 2 + 5)/2 $>$ Day 1

Cluster size	p_{FWE} (cluster)	Brain structure	x, y, z (mm)	SPM{T}
3,093	<.001	Right precuneus/retrosplenial cortex	18, -58, 23	9.73
		Left inferior parietal lobule	-36, -58, 50	8.99
		Right ANG	33, -61, 47	7.76
566	<.001	Left middle frontal gyrus	-27, -1, 56	5.64
			-45, 17, 35	5.59
144	.007	Left precentral gyrus	-45, 2, 41	5.60
		Left superior frontal gyrus	-27, 59, 8	5.75
119	.015		-21, 53, 2	5.68
		Left middle frontal gyrus	-39, 50, 5	4.33
94	.034	Right middle frontal gyrus	33, -1, 53	4.82
		Right superior frontal gyrus	27, 8, 50	4.62
		Left FFG/parahippocampal gyrus	-30, -46, -10	4.53
			-30, -58, -13	4.38
			-33, -40, -22	3.34

ANG = angular gyrus; FFG = fusiform gyrus; FWE = family-wise error; FWEc = family-wise error correction; SPM = Statistical Parametric Mapping.

SPM{T} contrast results are displayed at $p < .05$, FWE corrected at cluster level with an a priori search threshold of $p < .001$. FWEc = 94 voxels. Coordinates are given in MNI space.

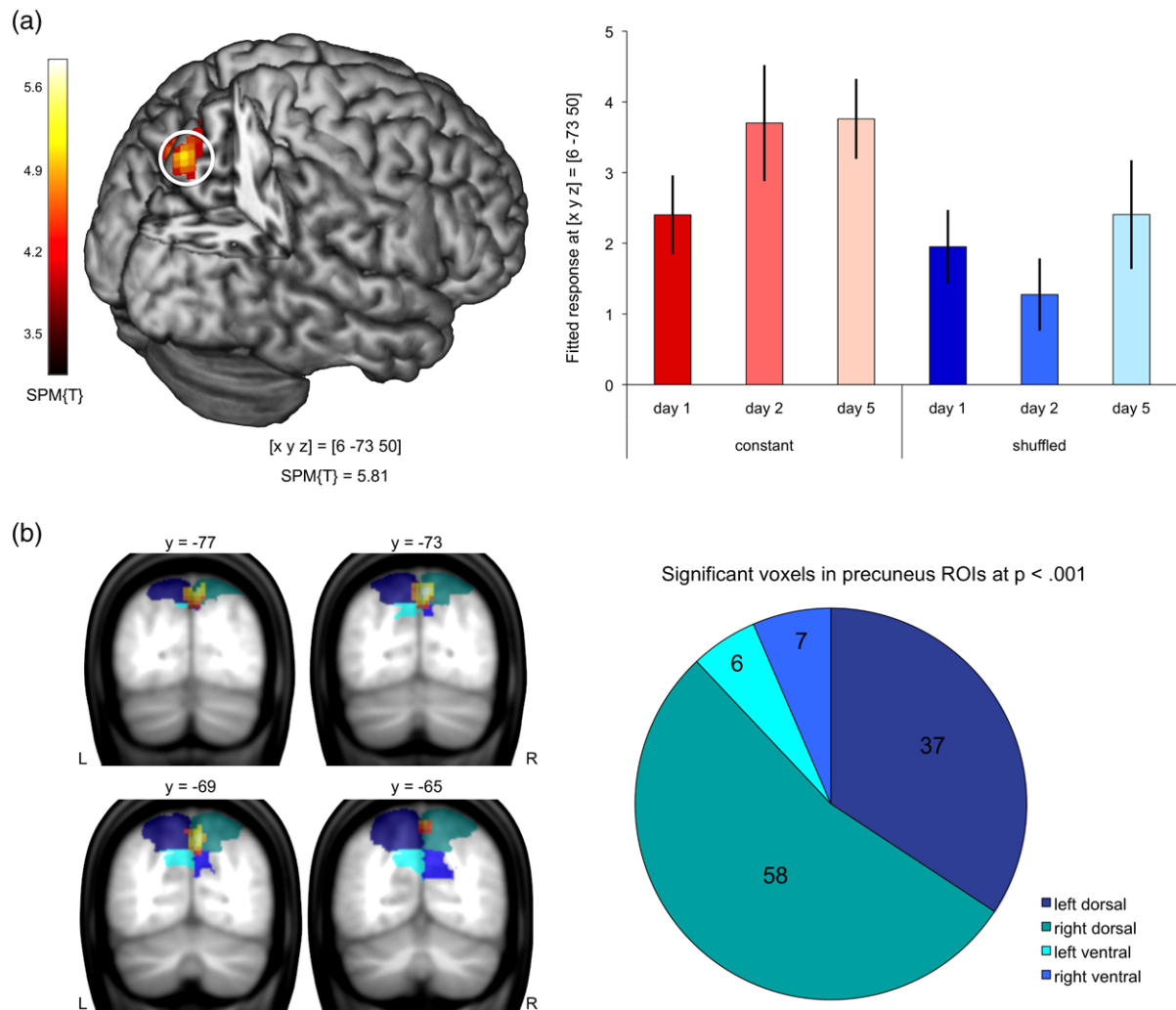


FIGURE 3 Activation of dorsal the precuneus during study of constant versus shuffled configurations. (a) Left panel: Activation cluster in the precuneus during study of constant versus shuffled configurations on Days 2 and 5, inclusively masked with the condition by day interaction contrast (local maximum at $[x, y, z] = [6, -73, 50]$; $p < .05$, FWE-corrected at cluster level with an initial search threshold of $p < .001$, uncorrected). Right panel: Bar plots depict mean BOLD signal (fitted and adjusted responses) at $[x, y, z] = [6, -73, 50] \pm SE$, separated by condition (constant vs. shuffled) and day (1, 2, and 5). (a) Localization of the activation cluster in the precuneus onto combined anatomical and literature-based ROIs. Left panel: Representative coronal sections depicting the activation cluster ($p < .05$, FWE-corrected at cluster level, initial search threshold = $p < .001$; uncorrected) in relation to the extent of the ROIs. Right panel: Number of voxels located in the four precuneus ROIs (dorsal vs. ventral \times left vs. right)

configurations that were later remembered (hippocampus: $SPM\{T\} = 4.21$; $p = .004$, small-volume FWE corrected; precuneus: $SPM\{T\} = 4.00$; $p = .020$, small-volume FWE corrected; see Figure 4, left panel). No significant activations were observed in the left dorsal or in the ventral precuneus (Figure 4, left panel). A masking analysis further revealed that the cluster in the precuneus that dissociated subsequently remembered and forgotten icon positions was among the precuneus regions that showed condition-independent RE from Day 1 to 5. While this DM effect (Paller et al., 1987) was statistically a main effect, hippocampal responses to subsequently recalled configurations were lower on Days 2 and 5 compared to Day 1 in the constant condition, but stayed at a similar magnitude across days in the shuffled condition. Precuneus responses peaked on Day 2 in the constant condition and increased over days in the shuffled condition (Figure 4, right panel).

TABLE 4 Activations associated with repeated presentation of the constant versus shuffled configurations (constant > shuffled, Days 2 + 5, no masking applied)

Cluster size	p_{FWE} (cluster)	Brain structure	x, y, z (mm)	$SPM\{T\}$
770	<.001	Left calcarine/inferior occipital gyrus	-3, -97, -7	6.13
		Right lingual gyrus	9, -94 -7	5.98
		Left calcarine/cuneus	-3, -100, 5	5.68
268	<.001	Right precuneus	6, -73, 50	5.81
		Precuneus/cuneus	0, -70, 32	4.05

FWE = family-wise error; FWEc = family-wise error correction; SPM = Statistical Parametric Mapping.

$SPM\{T\}$ contrast results are displayed at $p < .05$, FWE corrected at cluster level with an a priori search threshold of $p < .001$. FWEc = 268 voxels. Coordinates are given in MNI space.

An exploratory analysis at the whole-brain level ($p < .001$, uncorrected, minimum cluster size $k = 10$ voxels) revealed only the aforementioned activation clusters in the left hippocampus and right precuneus (Table 5). At a more liberal search threshold of $p < .005$, $k = 10$ voxels, we additionally observed a subsequent memory effect in the left dorsal precuneus ($[x, y, z] = [-9, -67, 53]$, $T = 3.26$) and in the left lateral occipital cortex ($[x, y, z] = [-33, -85, 23]$, $T = 2.96$).

3.2.4 | Precuneus activity and delayed memory performance

To explore the possibility that the learning network identified in this study might predict performance after a delay of 5 days, we computed a Spearman correlation between the peak brain response in the precuneus (contrasts constant vs. shuffled on Days 2 and 5) and the difference of recognition rates between constant and shuffled configurations in the test phase of the delayed memory test that was performed 5 days after the last learning day. We observed a positive correlation ($\rho = .408$; $p = .010$, one-tailed) and when further controlling for bivariate outliers using Shepherd's P_i correlation, the correlation remained significant at a one-tailed significance level ($\pi = .392$; $p = .036$, one-tailed; see Figure 5).

3.2.5 | Condition-dependent functional connectivity of the precuneus

To identify the networks that interact with the precuneus during learning of spatial configurations over time, we computed a functional

connectivity analysis using the PPI approach with the precuneus as seed region and the experimental condition (constant minus shuffled spatial configurations on Days 2 and 5) as psychological variable (see Section 2 for details). During study of constant as compared to shuffled configurations, we observed increased functional connectivity between the precuneus and a distributed parieto-occipito-temporal network ($p < .05$, FWE corrected at cluster level with an a priori search threshold of .001, uncorrected; Figure 6a). This network included the occipitoparietal cortex bilaterally (particularly bilateral superior and middle occipital gyrus, corresponding to visual areas V2 and V3) as well as bilateral occipitotemporal brain regions, most prominently the bilateral fusiform gyrus (FFG) as well as the right parahippocampal cortex, as determined with the SPM Anatomy Toolbox (Caspers et al., 2013, 2014; Eickhoff et al., 2005) (Figure 6b; Table 6). In the right hemisphere, the occipitotemporal cluster of learning-related functional connectivity with the dorsal precuneus extended into the anterior hippocampus proper as identified with the AAL ROI obtained from the WFU PickAtlas ($[x, y, z] = [-33, -19, -19]$; $t = 3.53$; $p = .040$, small-volume FWE corrected at voxel level; see Figure 6c). As shown in Figure 6c (right panel), higher functional connectivity between the precuneus and right hippocampus during study of constant versus shuffled configurations was observable on Days 2 and 5, but not on Day 1.

In an exploratory analysis, we inclusively masked the PPI contrast with the *novelty* and *familiarity* contrasts reported above (mask thresholded at $p < .05$, cluster-level FWE corrected with a priori threshold

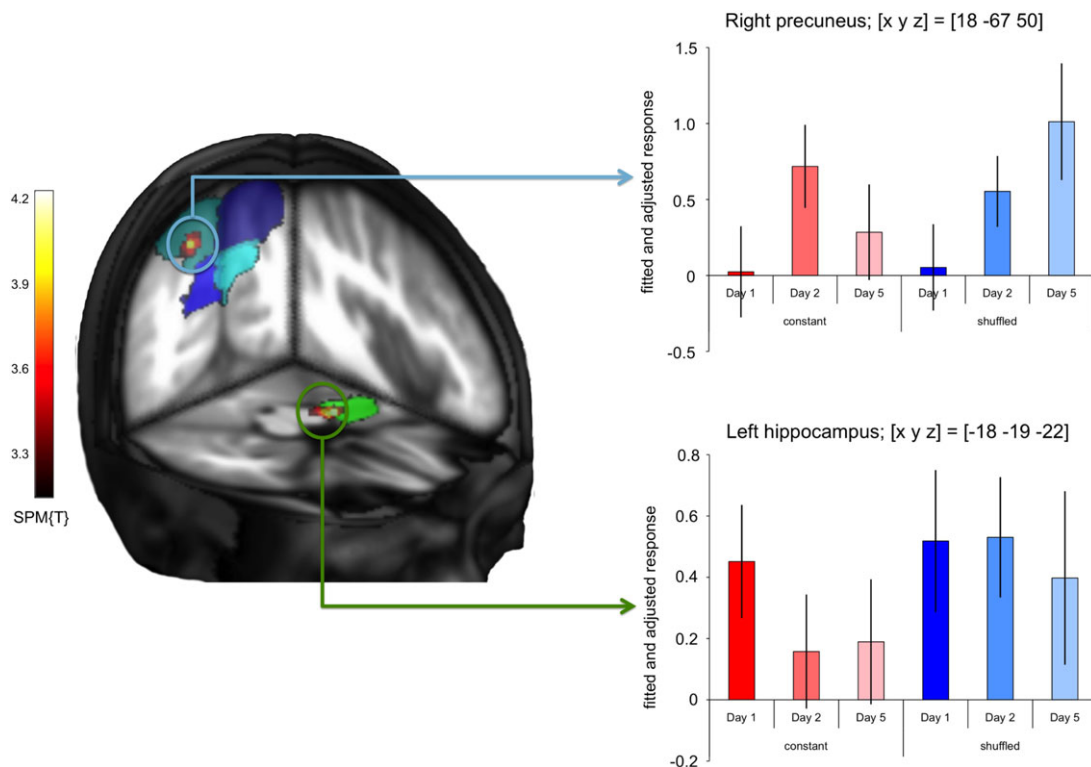


FIGURE 4 Neural correlates of successful encoding. Left panel: Group-level t contrast on the single-subject comparisons of subsequently remembered versus subsequently forgotten configurations ($p < .01$, small-volume FWE corrected at voxel level with an initial search threshold of $p < .001$, uncorrected). Activations are superimposed on the ROIs of the precuneus (blue, turquoise) and of the hippocampus (green), respectively. Right panel: Bar plots depict mean BOLD signal (fitted and adjusted responses) at the peak voxels in the precuneus (top; $[x, y, z] = [18, -67, 50]$) and hippocampus (bottom; $[x, y, z] = [-18, -19, -22]$) \pm SE, separated by condition (constant vs. shuffled) and day (1, 2, and 5)

TABLE 5 Activations associated with successful encoding of icon positions (remembered > forgotten), separated by condition and day

Cluster size	p_{FWE} (cluster)	Brain structure	x, y, z (mm)	SPM{T}
13	n/a	Left hippocampus	-18, -19, -22	4.21
14	n/a	Right precuneus	18, -67, 50	3.89

SPM{T} contrast results are displayed at a threshold of $p < .001$, uncorrected, minimum cluster size $k = 10$ voxels. Coordinates are given in MNI space.

$p < .001$, uncorrected). This approach revealed considerable overlap of the occipitoparietal and inferior temporal brain structures that showed increased learning-related functional connectivity with the precuneus with those that showed increased responses to familiar stimuli (i.e., Day 2 and Day 5 > Day 1). On the other hand, no overlap of the PPI contrast with the *novelty* contrast was observed.

4 | DISCUSSION

Using a spatial item-location learning paradigm conducted over five consecutive days, we have identified the precuneus as a key structure in the formation of complex spatial long-term memory traces. The extensive connectivity increase between the precuneus and a distributed parieto-occipito-temporal cortical network during gradual memory acquisition suggests that the precuneus plays a central role in a network that mediates visuospatial long-term memory.

4.1 | Parietal contributions to long-term memory encoding and retrieval

Participants were able to successfully encode the icon positions in the constant condition, with pronounced improvement from Day 1 to

2 and a slower learning curve from Day 2 to 5 (see Discussion, Supporting Information). This improvement was reflected by activation of the precuneus during study of constant versus shuffled configurations from Day 2 onward. Our results are in line with the recently proposed PMN (Gilmore et al., 2015) and expand the concept of the PMN by demonstrating that the precuneus is involved in the gradual acquisition of complex spatial information. A defining response characteristic of the PMN is RE, that is, increasing neural responses to repeated stimuli (Gilmore et al., 2015), and precuneus RE is particularly pronounced when familiarity is explicitly attended to (Kafkas & Montaldi, 2014). RE has previously been suggested to reflect a complementary phenomenon to the more extensively investigated repetition suppression (RS), that is, decreasing neural responses to repeated stimuli (Desimone, 1996; Gotts, Chow, & Martin, 2012). In the present study, both RS and RE were observed in response to item familiarity, and RE was widespread in the parietal lobes (Table 3). Location-specific RE (constant vs. shuffled) was, however, confined to a cluster in the dorsal precuneus (Figure 3, Table 4) that was located more dorsally than the parietal structures considered as part of the PMN (McDermott, Gilmore, Nelson, Watson, & Ojemann, 2017).

Similar to the results of the present study, Giesbrecht, Sy, and Guerin (2013) and Brodt et al. (2016) also reported RE in the precuneus in response to repeated spatial information. The precuneus activation in response to constant versus shuffled configurations bears a certain similarity to the medial parietal responses observed in a recent navigation-based spatial memory study, in which memory formation for locations was tested during navigation in a constant versus a randomly changing virtual reality environment (Brodt et al., 2016). In that study, a medial parietal cluster extending into the precuneus was increasingly active during repeated encounter of landmarks in a constant, but not in a changing environment. However, as that study was based on a navigation task, encoding success and memory retrieval

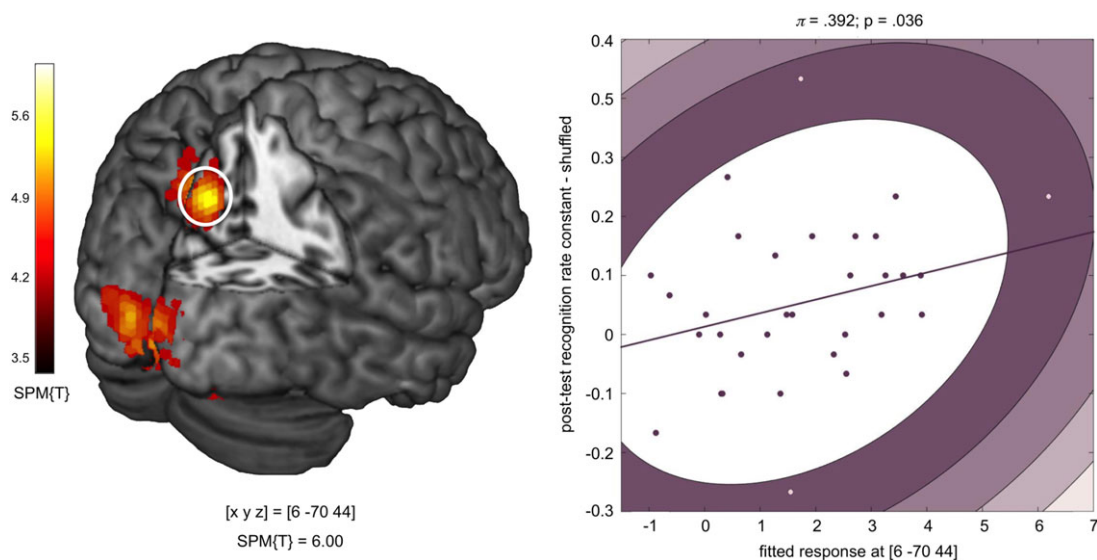


FIGURE 5 Correlation of precuneus activation and delayed memory performance. Left panel: Group-level t contrast on the single-subject comparisons of constant vs. shuffled configurations on Days 2 and 5 ($p < .05$, FWE corrected at cluster level, search threshold = $p < .001$, uncorrected). Right panel: Positive correlation between precuneus BOLD signal (parameter estimates at $[x, y, z] = [6, -70, 44]$) and difference in recognition performance for constant versus shuffled configurations in the delayed memory test. The plot depicts an outlier-robust Shepherd's Pi correlation (Schwarzkopf et al., 2012)

were tested indirectly, that is, by measuring the efficiency in the search for targets as a function of repeated encounter. In the present study, we instead focused on distinct encoding episodes that were subsequently intentionally retrieved in a designated task, thereby allowing for the computation of a subsequent memory effect. As shown in Figure 4, precuneus activation was more pronounced for remembered compared to forgotten configurations, supporting the notion that its activation actually reflected successful encoding. The difference in study design might be the reason for the more focused activation of the dorsal precuneus, particularly in the right hemisphere found in the current study (Figures 3b and 4), compared to the more extensive parietal activations observed by Brodt et al. Conversely, it is likely that the more extensive activation reported by Brodt et al., which included ventral parts of the precuneus, might be attributable to mnemonic processes beyond encoding, such as, particularly context-rich episodic, retrieval (Wagner et al., 2005; Ciaramelli et al., 2008).

4.2 | Representation of visuospatial information in the precuneus

One potentially unifying explanation for the engagement of the precuneus in visuospatial attention (Corbetta, Patel, & Shulman, 2008) and search processes (Allen, Humphreys, & Matthews, 2008; Pollmann et al., 2003), on the one hand, and in memory processes like episodic retrieval (Vilberg & Rugg, 2008) and visuospatial memory formation (Figure 4; see also Uncapher & Rugg, 2009; Brodt et al., 2016), on the other hand, could be its well-documented role in visual imagery (Byrne et al., 2007; Cavanna & Trimble, 2006; Fletcher et al., 1995). Activation of the precuneus during imagery is particularly pronounced when visual mnemonic representations exist (Buckner et al., 1996), for example, during imagery of famous faces (Ishai, Haxby, & Ungerleider, 2002), or of specific, previously presented, objects as compared to generic representations of objects (Handy et al., 2004). Visual imagery as a likely candidate cognitive process underlying precuneus involvement in mnemonic processing is also compatible with a recent study of retrieval using stimuli highly similar to the ones employed here (Richter, Cooper, Bays, & Simons, 2016). In that study, retrieval-related precuneus activity correlated with subjective vividness of retrieved episodes rather than overall retrieval success or precision.

While our results, together with recent research on navigation-based memory formation (Brodt et al., 2016), the retrieval of well-consolidated spatial information (Sommer, 2017; Takashima et al., 2007; van Buuren et al., 2014), and vividness of retrieved visuospatial memory traces (Richter et al., 2016), convergingly point to a critical role for the precuneus in memory for complex visuospatial information, a more domain-general role for the precuneus in associative memory cannot be excluded, as precuneus involvement in episodic retrieval is a well-replicated finding, irrespective of stimulus material (Vilberg & Rugg, 2008). With respect to encoding, Uncapher and Wagner (2009) also reported parietal subsequent memory effects for several different types of stimuli. Nevertheless, numerous previous studies have implicated the precuneus in visuospatial attention and search processes (Allen et al., 2008; Corbetta et al., 2008; Giesbrecht

et al., 2013; Pollmann et al., 2003). Notably, Giesbrecht et al. (2013) could demonstrate that the precuneus response during visual search is sensitive to repetition effects, with the SPL/precuneus exhibiting learning-related RE. Conversely, in a study of attention-dependent modulation of episodic encoding, Uncapher and Rugg (2009) observed a specific subsequent memory effect for attended, but not unattended locations of objects. It is therefore plausible to assume that, even though the function of the precuneus in long-term memory most likely extends beyond visuospatial processing, visuospatial memory traces may be particularly suitable for gradual strengthening via precuneus RE.

The precuneus, together with the adjacent PCC is considered part of the DMN (Raichle et al., 2001; Buckner et al., 2008; Leech, Kamourieh, Beckmann, & Sharp, 2011), and one might argue that increasing precuneus activation during presentation of constant versus shuffled configurations merely reflects increasing DMN activity in the “easier” condition. Importantly, though, the PMN is, despite its close proximity, at least partly anatomically dissociable from the DMN (Gilmore et al., 2015), and particularly the dorsal precuneus also exhibits pronounced functional connectivity with the right frontoparietal network (rFPN), a task-positive network implicated in attention and visual working memory (Leech et al., 2011; Utevsky, Smith, & Huettel, 2014). Notably, Utevsky et al. (2014) identified one cluster within the precuneus that exhibited both resting-state connectivity with the DMN and task-related connectivity with the rFPN, and this cluster was in close proximity to the precuneus region identified in the present study (peak voxel at $[x, y, z] = [6, -63, 42]$). Furthermore, we have previously demonstrated that the hippocampus exhibits task-specific modulation of functional connectivity with the DMN and the rFPN during explicit memory formation. While left hippocampal-DMN functional connectivity increases during deep (self-relevant) encoding, right hippocampal-rFPN connectivity is more pronounced during shallow, nonsemantic encoding (Schott et al., 2013). The dorsal precuneus was among the few brain regions that showed an overlap of the two connectivity patterns. Future studies should directly compare precuneus activation patterns during different encoding tasks and for different stimulus types and consider potential regional specializations within the precuneus (Utevsky et al., 2014).

It remains, as of now, an open question, how the response pattern of the precuneus to successfully encode *shuffled* configurations should be interpreted. Specifically, shuffled configurations elicited an increasing positive subsequent memory effect from Day 1 to 5 (Figure 4). One possibility would be suggest that the strengthening of item representations, which was also possible in the shuffled condition, may to some extent have contribute to successful encoding of at least a small subgroup of the configurations, which was in turn reflected by more pronounced precuneus RE for subsequently remembered configurations (Gilmore et al., 2015). On the other hand, the subsequent memory effect in the hippocampus remained high in the shuffled condition, possibly due to continued associative novelty (Davachi, 2006). Studies using longer learning periods (Sommer, 2017) may help to further elucidate how the precuneus responds to repeatedly changing configurations of increasingly familiar items.

4.3 | Can encoding and retrieval processes in parietal cortices be separated?

Neocortical learning processes—unlike hippocampus-dependent memory—almost invariably require multiple encoding episodes (Henke, 2010). A fundamental limitation inherent to all encoding studies using multiple learning episodes, however, is that encoding and retrieval events can hardly be completely separated. Along this line, one might argue that the precuneus response to constant configurations, similarly to the previously described medial parietal activations related to a constant versus changing environment (Brodtt et al.,

2016), might reflect more detailed or vivid retrieval (Richter et al., 2016) rather than the actual acquisition of new memory traces. Indeed, a selective role for parietal structures in retrieval rather than encoding might be inferred from the encoding–retrieval flip described for the PMN, that is, a negative subsequent memory effect is followed by subsequent RE (Gilmore et al., 2015). However, in the present study, the dorsal precuneus did exhibit RE (Figure 3), but this RE was accompanied by a *positive* subsequent memory effect, albeit primarily for at least partly familiar information, as indexed by the largely absent subsequent memory effect on Day 1 (Figure 4). Furthermore,

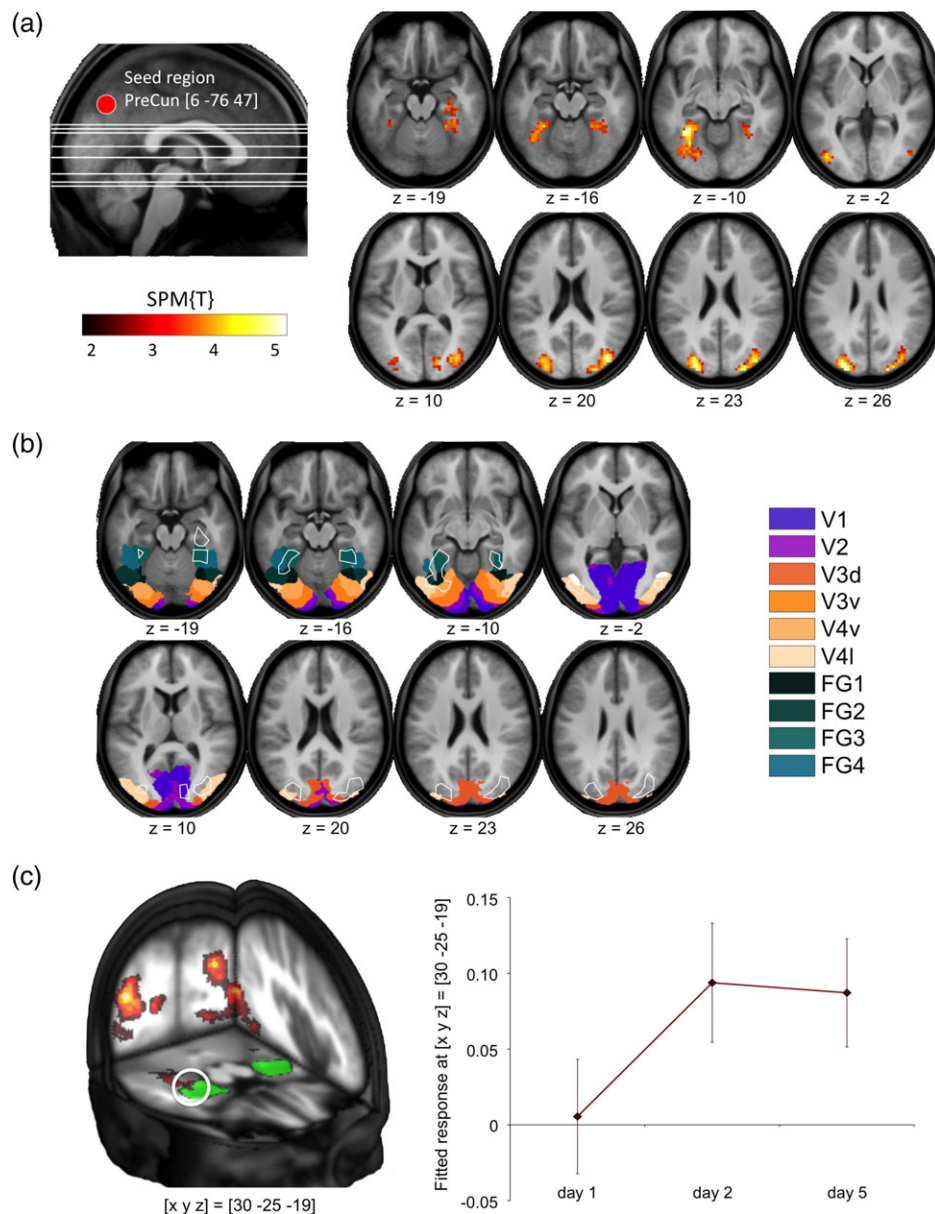


FIGURE 6 Condition-dependent modulation of precuneus functional connectivity. (a) During study of constant versus shuffled configurations, the precuneus exhibited increased functional connectivity with an extensive parieto–occipito–temporal network. Left panel: Representative volume of interest in the precuneus. Right panel: Brain regions with increased precuneus functional connectivity during study of constant versus shuffled configurations. (b) Overlaying the clusters of condition-dependent functional connectivity onto probabilistic cytoarchitectonic maps (Caspers et al., 2013, 2014; Eickhoff et al., 2005) revealed that the network included extrastriate cortices and large portions of the ventral and also dorsal visual stream. (c) Left panel: Increased activity-dependent functional connectivity of the precuneus during study of constant versus shuffled configurations extended into the right hippocampus, as delineated with the ROI from the SPM Anatomy Toolbox (green). Right panel: Plots depict increase of functional connectivity between the precuneus and the right hippocampus from Day 1 to 5 (fitted response \pm SE)

TABLE 6 Condition-dependent functional connectivity of the precuneus (PPI results)

Cluster size	p_{FWE} (cluster)	Brain structure	x, y, z (mm)	SPM{T}
459	<.001	Left FFG	-33, -52, -10	4.99
		Left superior occipital gyrus	-24, -88, 26	4.82
		Left inferior occipital gyrus	-42, -79, 2	4.42
285	<.001	Right middle occipital gyrus	39, -79, 20	4.92
			30, -82, 11	4.17
		Right superior occipital gyrus	27, -88, 23	4.54
97	.019	Right FFG	24, -46, -16	3.87
			36, -43, -16	3.82
		Right parahippocampal gyrus	30, -25, -19	3.71

FFG = fusiform gyrus; FWE = family-wise error; FWEc = family-wise error correction; PPI = psychophysiological interaction; SPM = Statistical Parametric Mapping.

PPI results are displayed at $p < .05$, FWE corrected at cluster level with an a priori search threshold of $p < .001$. FWEc = 97 voxels. Coordinates are given in MNI space.

precuneus activation to constant configurations on Days 2 and 5 correlated with better memory performance for constant configurations even 5 days after the main study phase (Figure 5). Therefore, our results suggest that, beyond vividness or detailed retrieval, the dorsal precuneus is most likely also engaged in the gradual encoding of spatial associative memory representations.

The observed response pattern of the dorsal precuneus with RE during repeated exposure (Figure 3; see also Vilberg & Rugg, 2008; Gilmore et al., 2015), and a positive subsequent memory effect for successfully encoded icon positions from Day 2 onward (Figure 4; see also Uncapher & Rugg, 2009; Brodt et al., 2016), may reflect the often underappreciated difficulty in clearly dichotomizing encoding and retrieval processes. With respect to the present study, it is conceivable that the encoding of constant compared to shuffled configurations does, from Day 2 onward, also qualify as a retrieval event, for example, by means of automatic reactivation of associated information (Khader et al., 2007). Considering that participants knew that they would later be probed on the icon positions, they may have—voluntarily or involuntarily—retrieved the information encoded on the previous study days in order to improve their performance (Karpicke and Roediger, 2008; Khader et al., 2007; Richardson-Klavehn, 2010). Notably, at the behavioral level, repeated retrieval of mnemonic information (i.e., retrieval practice) has been shown to promote long-term encoding success (e.g., Karpicke and Roediger, 2008). Neuroimaging studies of the retrieval practice effects using vocabulary learning (van den Broek, Takashima, Segers, Fernandez, & Verhoeven, 2013) or paired associate verbal memory tasks (Nelson, Arnold, Gilmore, & McDermott, 2013; Wing, Marsh, & Cabeza, 2013) have actually shown that retrieval practice elicits parietal, including precuneus activations, and the precuneus (van den Broek et al., 2013) and adjacent, more lateral, parietal cortices (Nelson et al., 2013) were among the brain regions in which practice-related activation was associated with successful encoding. Notably, Nelson et al. demonstrated that, once participants had performed retrieval practice for a subset of study items, subsequent further study of these items elicited parietal RE (Nelson et al., 2013). Furthermore, Zeithamova et al. reported that

the formation of new associative mnemonic representations was accompanied by functional connectivity increases between the hippocampus and the mPFC, and also the precuneus (Zeithamova, Dominick, & Preston, 2012). Together with our present results, those findings raise the possibility that parietal RE may constitute a neural underpinning of the behavioral retrieval practice effect.

4.4 | A parieto-occipito-temporal network supports visuospatial long-term memory

While increased brain responses to constant compared to shuffled configurations were largely restricted to the precuneus, our PPI analysis further revealed that the precuneus exhibited increased functional connectivity with a distributed network of parietal, occipital, and temporal neocortical regions, including visual areas V2 and V3 (Wilms et al., 2010) and inferior occipito-temporal cortices comprising the FFG and parahippocampal gyrus (Figure 6b). Several of these structures have previously been identified as belonging to the dorsal and ventral visual stream, two anatomically distinct higher order visual modules that have been suggested to separately process object-related and spatial aspects of visual information (Kravitz, Saleem, Baker, & Mishkin, 2011; Mishkin, Ungerleider, & Macko, 1983). There was considerable overlap between the cortical regions that exhibited increased learning-related functional connectivity with the precuneus and those that showed condition-independent RE from Day 1 to 5. As precuneus RE was location-specific and RE in parietal regions has been suggested to reflect the formation of novel networks (Gilmore et al., 2015; Henson, Shallice, & Dolan, 2000; Segaert et al., 2013), our results raise the possibility that, while complex visual information elicits widespread familiarity-related RE in stimulus-responsive brain structures, the precuneus may gradually integrate such information with respect to spatial detail, as indexed by its location-specific RE. Along this line, an earlier functional connectivity study of the FFG during retrieval of well-learned face-location associations revealed increased functional coupling between the FFG and the precuneus (Takashima et al., 2007). The precuneus may therefore be considered a potential hub region that mediates the integration of distributed visuospatial information into a more holistic representation. One could further speculate that the familiarity responses may to some extent reflect the Gestaltists' notion that "the whole is more than the sum of its parts," which has been suggested to also apply to visual cognition (Bartolomeo, Vuilleumier, & Behrmann, 2015): When a configuration is encoded and—presumably—sets the stage for a new representation, the repeated concurrent occurrence of its elements may engage additional brain structures involved in stimulus processing—such as the FFG, which contributes to object representation—thereby reflecting the overarching comprehension of items belonging together and forming a whole.

4.5 | Hippocampal and neocortical contributions to long-term associative memory

An important question is how the precuneus, and potentially additional parietal neocortical regions (Gilmore et al., 2015), interact with the MTL memory system and to what extent a parietal lobe memory system might operate independently. In their navigation study, Brodt et al. (2016)

reported that familiarity-related response increases in the precuneus were accompanied by reduced hippocampal responses. Similarly, Kafkas and Montaldi (2014) systematically varied the instruction of a visual learning task, requesting participants to either rate the novelty or the familiarity of (the same set of) stimuli, and identified the hippocampal formation as a novelty-responsive region showing RS, whereas the precuneus was familiarity-sensitive and exhibited RE. Notably, the precuneus region identified by Kafkas and Montaldi was in very close proximity to the one found in our study. Also in the present study, RS was observed in the hippocampus, but independently of condition (constant vs. shuffled). The hippocampus did nevertheless activate as a function of successful encoding, and the hippocampal subsequent memory effect decreased from Day 1 to 5 for constant, but not shuffled, configurations (Figure 4). The hippocampus was also among the brain structures that exhibited increased learning-related functional connectivity with the precuneus on Days 2 and 5 (Figure 6c). In line with the notion that the hippocampus is capable of single-trial memory formation, while neocortical encoding processes require multiple encoding episodes (Henke, 2010), the hippocampus thus contributed to successful encoding of the stimuli on a trial-by-trial basis, while the gradual strengthening of the studied configurations over time was mediated by the precuneus as primary integrator. Our results thus support the notion that the hippocampus and the precuneus exhibit different neural response profiles during long-term memory formation (see also, e.g., Uncapher & Rugg, 2009).

While the observed slow and gradual acquisition of location-specific information in the dorsal precuneus is thus compatible with the general concept of fast, hippocampus-dependent as opposed to slow, neocortical encoding (Henke, 2010), it should be mentioned that there may be exceptions to this distinction. Particularly, the mPFC has been implicated in the integration of novel information into preexisting representations (van Kesteren et al., 2012), and this form of neocortical encoding can occur rapidly and during encoding episodes, for example during insight-based learning (Kizilirmak, Thuerich, Folta-Schoofs, Schott, & Richardson-Klavehn, 2016). While we did not find mPFC activation during processing or successful encoding of constant configurations (see Results, Supporting Information), we cannot exclude the possibility that mPFC involvement in encoding might have occurred after prolonged study and thus long-term consolidation of the configurations, possibly enabling the rapid encoding of additional information into the stabilized representations (Sommer, 2017).

5 | LIMITATIONS

A limitation of our study arises from the unintended nonrandom presentation of the background images during the familiarization phase (see Section 2, first footnote). As a result of this lapse, there was a small, but significant recognition advantage for (subsequently) constant configurations already on Day 1, which was related to the temporal position of the background pictures in the familiarization phase. Interestingly, this advantage was most likely not caused by simple primacy or recency effects (see Results and Figure S1, Supporting Information). Despite this performance difference on Day 1, we could nevertheless demonstrate substantially higher learning in the constant compared to the shuffled condition only, as evident from the highly

significant difference between the learning rates of the two conditions (see Section 3 for details). Regarding our fMRI results, we cannot exclude an effect of the nonrandom presentation of the background images on activations in secondary visual areas, but, importantly, there was no difference in precuneus activation between the two conditions on the first day, even at most liberal statistical thresholds (see Results and Discussion, Supporting Information).

Furthermore, the rather parsimonious design of the delayed memory test must be considered as a limitation. With the substitution of the icon probed in the last test session of the main experiment, we aimed to test for both the successful encoding and the flexibility of the encoded mnemonic traces (Driscoll, Pettit, Minderer, Chettih, & Harvey, 2017). The rather low task performance in both conditions (Figure 1 and Table 1; Table S5, Supporting Information), however, suggests that the task may simply have been too difficult, resulting in incomplete consolidation even in the constant condition. While a positive correlation between delayed memory performance and precuneus activation (Figure 5) may be considered further evidence for an important role of the precuneus in associative visuospatial memory, although it must be cautioned that some authors have raised concerns about the power of correlations even at moderately large sample sizes (Yarkoni, 2009; see Discussion, Supporting Information).

6 | CONCLUSIONS

The present study shows that the precuneus likely acts as a core structure in a distributed neocortical network that supports the encoding of complex visuospatial information into long-term memory. Our results also highlight the potential role of parietal cortices and of the brain's midline structures as a neocortical memory network that may operate complementarily to the MTL memory system or, at least in part, even independently of the hippocampus.

ACKNOWLEDGMENTS

The authors would like to thank all volunteers for taking part in this time-consuming study. The authors further thank Denise Scheermann, Geertje Wank, and Claus Tempelmann for their assistance with MRI acquisition. The authors would also like to thank two anonymous reviewers for their very helpful and constructive comments that have helped us to considerably improve the manuscript. This work was supported by the Deutsche Forschungsgemeinschaft (DFG SFB 779, TP A04, A08, A10, B14), and the Leibniz-Gemeinschaft (Pakt für Forschung und Innovation).

AUTHOR CONTRIBUTIONS

B.H.S. designed research with support from E.L., C.S., and A.R.-K.; B.H.S., E.L., and I.-M.P. performed the research; B.H.S. and T.W. analyzed the data; B.H.S., T.W., J.M.K., A.R., C.S., S.P., and A.R.-K. wrote the paper.

ORCID

Björn H. Schott  <https://orcid.org/0000-0002-8237-4481>

REFERENCES

- Allen, H. A., Humphreys, G. W., & Matthews, P. M. (2008). A neural marker of content-specific active ignoring. *Journal of Experimental Psychology. Human Perception and Performance*, *34*, 286–297.
- Barman, A., Richter, S., Soch, J., Deibele, A., Richter, A., Assmann, A., ... Schott, B. H. (2015). Gender-specific modulation of neural mechanisms underlying social reward processing by autism quotient. *Social Cognitive and Affective Neuroscience*, *10*, 1537–1547.
- Bartolomeo, P., Vuilleumier, P., & Behrmann, M. (2015). The whole is greater than the sum of the parts: Distributed circuits in visual cognition. *Cortex*, *72*, 1–4.
- Brodts, S., Pohlchen, D., Flanagin, V. L., Glasauer, S., Gais, S., & Schonauer, M. (2016). Rapid and independent memory formation in the parietal cortex. *Proceedings of the National Academy of Sciences of the United States of America*, *113*, 13251–13256.
- Buckner, R. L., Andrews-Hanna, J. R., & Schacter, D. L. (2008). The brain's default network: Anatomy, function, and relevance to disease. *Annals of the New York Academy of Sciences*, *1124*, 1–38.
- Buckner, R. L., Raichle, M. E., Miezin, F. M., & Petersen, S. E. (1996). Functional anatomic studies of memory retrieval for auditory words and visual pictures. *The Journal of Neuroscience*, *16*, 6219–6235.
- Byrne, P., Becker, S., & Burgess, N. (2007). Remembering the past and imagining the future: A neural model of spatial memory and imagery. *Psychological Review*, *114*, 340–375.
- Cabeza, R., Ciaramelli, E., Olson, I. R., & Moscovitch, M. (2008). The parietal cortex and episodic memory: An attentional account. *Nature Reviews Neuroscience*, *9*, 613–625.
- Cabeza, R., Dolcos, F., Prince, S. E., Rice, H. J., Weissman, D. H., & Nyberg, L. (2003). Attention-related activity during episodic memory retrieval: A cross-function fMRI study. *Neuropsychologia*, *41*, 390–399.
- Caspers, J., Zilles, K., Amunts, K., Laird, A. R., Fox, P. T., & Eickhoff, S. B. (2014). Functional characterization and differential coactivation patterns of two cytoarchitectonic visual areas on the human posterior fusiform gyrus. *Human Brain Mapping*, *35*, 2754–2767.
- Caspers, J., Zilles, K., Eickhoff, S. B., Schleicher, A., Mohlberg, H., & Amunts, K. (2013). Cytoarchitectonical analysis and probabilistic mapping of two extrastriate areas of the human posterior fusiform gyrus. *Brain Structure and Function*, *218*, 511–526.
- Cavanna, A. E., & Trimble, M. R. (2006). The precuneus: A review of its functional anatomy and behavioural correlates. *Brain*, *129*, 564–583.
- Ciaramelli, E., Grady, C. L., & Moscovitch, M. (2008). Top-down and bottom-up attention to memory: A hypothesis (AtoM) on the role of the posterior parietal cortex in memory retrieval. *Neuropsychologia*, *46*, 1828–1851.
- Corbetta, M., Kincade, J. M., & Shulman, G. L. (2002). Neural systems for visual orienting and their relationships to spatial working memory. *Journal of Cognitive Neuroscience*, *14*, 508–523.
- Corbetta, M., Patel, G., & Shulman, G. L. (2008). The reorienting system of the human brain: From environment to theory of mind. *Neuron*, *58*, 306–324.
- Davachi, L. (2006). Item, context and relational episodic encoding in humans. *Current Opinion in Neurobiology*, *16*, 693–700. <https://doi.org/10.1016/j.conb.2006.10.012>
- Desimone, R. (1996). Neural mechanisms for visual memory and their role in attention. *Proceedings of the National Academy of Sciences of the United States of America*, *93*, 13494–13499.
- Driscoll, L. N., Pettit, N. L., Minderer, M., Chettih, S. N., & Harvey, C. D. (2017). Dynamic reorganization of neuronal activity patterns in parietal cortex. *Cell*, *170*, 986–999.e16.
- Düzel, E., Bunzeck, N., Guitart-Masip, M., & Düzel, S. (2010). Novelty-related motivation of anticipation and exploration by dopamine (NOMAD): Implications for healthy aging. *Neuroscience and Biobehavioral Reviews*, *34*, 660–669.
- Efron, B., & Tibshirani, R. (1993). *An introduction to the bootstrap*. New York, NY: Chapman & Hall.
- Eickhoff, S. B., Stephan, K. E., Mohlberg, H., Grefkes, C., Fink, G. R., Amunts, K., & Zilles, K. (2005). A new SPM toolbox for combining probabilistic cytoarchitectonic maps and functional imaging data. *NeuroImage*, *25*, 1325–1335.
- Eklund, A., Nichols, T. E., & Knutsson, H. (2016). Cluster failure: Why fMRI inferences for spatial extent have inflated false-positive rates. *Proceedings of the National Academy of Sciences of the United States of America*, *113*, 7900–7905.
- Fletcher, P. C., Frith, C. D., Baker, S. C., Shallice, T., Frackowiak, R. S., & Dolan, R. J. (1995). The mind's eye—Precuneus activation in memory-related imagery. *NeuroImage*, *2*, 195–200.
- Friston, K. J., Buechel, C., Fink, G. R., Morris, J., Rolls, E., & Dolan, R. J. (1997). Psychophysiological and modulatory interactions in neuroimaging. *NeuroImage*, *6*, 218–229.
- Giesbrecht, B., Sy, J. L., & Guerin, S. A. (2013). Both memory and attention systems contribute to visual search for targets cued by implicitly learned context. *Vision Research*, *85*, 80–89.
- Gilmore, A. W., Nelson, S. M., & McDermott, K. B. (2015). A parietal memory network revealed by multiple MRI methods. *Trends in Cognitive Sciences*, *19*, 534–543.
- Gitelman, D. R., Penny, W. D., Ashburner, J., & Friston, K. J. (2003). Modeling regional and psychophysiological interactions in fMRI: The importance of hemodynamic deconvolution. *NeuroImage*, *19*, 200–207.
- Gotts, S. J., Chow, C. C., & Martin, A. (2012). Repetition priming and repetition suppression: A case for enhanced efficiency through neural synchronization. *Cognitive Neuroscience*, *3*, 227–237.
- Handy, T. C., Miller, M. B., Schott, B. H., Shroff, N. M., Janata, P., Van Horn, J. D., ... Gazzaniga, M. S. (2004). Visual imagery and memory: Do retrieval strategies affect what the mind's eye sees? *European Journal of Cognitive Psychology*, *16*, 631–652.
- Henke, K. (2010). A model for memory systems based on processing modes rather than consciousness. *Nature Reviews Neuroscience*, *11*, 523–532.
- Henson, R., Shallice, T., & Dolan, R. (2000). Neuroimaging evidence for dissociable forms of repetition priming. *Science*, *287*, 1269–1272.
- Herbert, M. C., Soch, J., Wüstenberg, T., Krauel, K., Pujara, M., Koenigs, M., ... Schott, B. H. (2016). A negative relationship between ventral striatal loss anticipation response and impulsivity in borderline personality disorder. *NeuroImage. Clinical*, *12*, 724–736.
- Hinrichs, H., Scholz, M., Tempelmann, C., Woldorff, M. G., Dale, A. M., & Heinze, H. J. (2000). Deconvolution of event-related fMRI responses in fast-rate experimental designs: Tracking amplitude variations. *Journal of Cognitive Neuroscience*, *12*(Suppl. 2), 76–89.
- Hutchinson, J. B., Uncapher, M. R., & Wagner, A. D. (2009). Posterior parietal cortex and episodic retrieval: Convergent and divergent effects of attention and memory. *Learning & Memory*, *16*, 343–356.
- Ishai, A., Haxby, J. V., & Ungerleider, L. G. (2002). Visual imagery of famous faces: Effects of memory and attention revealed by fMRI. *NeuroImage*, *17*, 1729–1741.
- Kafkas, A., & Montaldi, D. (2014). Two separate, but interacting, neural systems for familiarity and novelty detection: A dual-route mechanism. *Hippocampus*, *24*, 516–527.
- Karipke, J. D., & Roediger, H. L., III. (2008). The critical importance of retrieval for learning. *Science*, *319*, 966–968.
- Khader, P., Knoth, K., Burke, M., Ranganath, C., Bien, S., & Rosler, F. (2007). Topography and dynamics of associative long-term memory retrieval in humans. *Journal of Cognitive Neuroscience*, *19*, 493–512.
- Kim, H. (2011). Neural activity that predicts subsequent memory and forgetting: A meta-analysis of 74 fMRI studies. *NeuroImage*, *54*, 2446–2461.
- Kizilirmak, J. M., Thuerich, H., Folta-Schoofs, K., Schott, B. H., & Richardson-Klavehn, A. (2016). Neural correlates of learning from induced insight: A case for reward-based episodic encoding. *Frontiers in Psychology*, *7*, 1693.
- Kravitz, D. J., Saleem, K. S., Baker, C. I., & Mishkin, M. (2011). A new neural framework for visuospatial processing. *Nature Reviews Neuroscience*, *12*, 217–230.
- Kriegeskorte, N., Lindquist, M. A., Nichols, T. E., Poldrack, R. A., & Vul, E. (2010). Everything you never wanted to know about circular analysis, but were afraid to ask. *Journal of Cerebral Blood Flow & Metabolism*, *30*, 1551–1557.
- Leech, R., Kamourieh, S., Beckmann, C. F., & Sharp, D. J. (2011). Fractionating the default mode network: Distinct contributions of the ventral and dorsal posterior cingulate cortex to cognitive control. *The Journal of Neuroscience*, *31*, 3217–3224.

- McDermott, K. B., Gilmore, A. W., Nelson, S. M., Watson, J. M., & Ojemann, J. G. (2017). The parietal memory network activates similarly for true and associative false recognition elicited via the DRM procedure. *Cortex*, *87*, 96–107.
- Mishkin, M., Ungerleider, L. G., & Macko, K. A. (1983). Object vision and spatial vision: Two cortical pathways. *Trends in Neurosciences*, *6*, 414–417.
- Morris, S. B., & DeShon, R. P. (2002). Combining effect size estimates in meta-analysis with repeated measures and independent-groups designs. *Psychological Methods*, *7*, 105–125.
- Nelson, S. M., Arnold, K. M., Gilmore, A. W., & McDermott, K. B. (2013). Neural signatures of test-potentiated learning in parietal cortex. *The Journal of Neuroscience*, *33*, 11754–11762.
- Nyberg, L. (2005). Any novelty in hippocampal formation and memory? *Current Opinion in Neurology*, *18*, 424–428.
- Paller, K. A., Kutas, M., & Mayes, A. R. (1987). Neural correlates of encoding in an incidental learning paradigm. *Electroencephalography and Clinical Neurophysiology*, *67*, 360–371.
- Pollmann, S., & von Cramon, D. Y. (2000). Object working memory and visuospatial processing: Functional neuroanatomy analyzed by event-related fMRI. *Experimental Brain Research*, *133*, 12–22.
- Pollmann, S., Weidner, R., Humphreys, G. W., Olivers, C. N., Muller, K., Lohmann, G., ... Watson, D. G. (2003). Separating distractor rejection and target detection in posterior parietal cortex—An event-related fMRI study of visual marking. *NeuroImage*, *18*, 310–323.
- Raichle, M. E., MacLeod, A. M., Snyder, A. Z., Powers, W. J., Gusnard, D. A., & Shulman, G. L. (2001). A default mode of brain function. *Proceedings of the National Academy of Sciences of the United States of America*, *98*, 676–682.
- Ranganath, C., & Rainer, G. (2003). Neural mechanisms for detecting and remembering novel events. *Nature Reviews. Neuroscience*, *4*, 193–202.
- Richardson-Klavehn, A. (2010). Priming, automatic recollection, and control of retrieval: Toward an integrative retrieval architecture. In J. H. Mace (Ed.), *The act of remembering* (pp. 11–179). Oxford, England: Wiley-Blackwell.
- Richter, F. R., Cooper, R. A., Bays, P. M., & Simons, J. S. (2016). Distinct neural mechanisms underlie the success, precision, and vividness of episodic memory. *eLife*, *5*, e18260.
- Rieger, J. W., Gegenfurtner, K. R., Schalk, F., Koechy, N., Heinze, H. J., & Grueschow, M. (2013). BOLD responses in human V1 to local structure in natural scenes: Implications for theories of visual coding. *Journal of Vision*, *13*, 19.
- Rugg, M. D., Otten, L. J., & Henson, R. N. (2002). The neural basis of episodic memory: Evidence from functional neuroimaging. *Philosophical Transactions of the Royal Society of London. Series B, Biological Sciences*, *357*, 1097–1110.
- Rousselet, G. A., & Pernet, C. R. (2012). Improving standards in brain-behavior correlation analyses. *Frontiers in Human Neuroscience*, *6*, 119.
- Schott, B. H., Wüstenberg, T., Wimber, M., Fenker, D. B., Zierhut, K. C., Seidenbecher, C. I., ... Richardson-Klavehn, A. (2013). The relationship between level of processing and hippocampal-cortical functional connectivity during episodic memory formation in humans. *Human Brain Mapping*, *34*, 407–424.
- Schubert, R., Ritter, P., Wüstenberg, T., Preuschhof, C., Curio, G., Sommer, W., & Villringer, A. (2008). Spatial attention related SEP amplitude modulations covary with BOLD signal in S1—A simultaneous EEG-fMRI study. *Cerebral Cortex*, *18*, 2686–2700.
- Schwarzkopf, D. S., De Haas, B., & Rees, G. (2012). Better ways to improve standards in brain-behavior correlation analysis. *Frontiers in Human Neuroscience*, *6*, 200.
- Segaert, K., Weber, K., de Lange, F. P., Petersson, K. M., & Hagoort, P. (2013). The suppression of repetition enhancement: A review of fMRI studies. *Neuropsychologia*, *51*, 59–66.
- Sestieri, C., Shulman, G. L., & Corbetta, M. (2017). The contribution of the human posterior parietal cortex to episodic memory. *Nature Reviews. Neuroscience*, *18*, 183–192.
- Soch, J., Deserno, L., Assmann, A., Barman, A., Walter, H., Richardson-Klavehn, A., & Schott, B. H. (2017). Inhibition of information flow to the default mode network during self-reference versus reference to others. *Cerebral Cortex*, *27*, 3930–3942.
- Sommer, T. (2017). The emergence of knowledge and how it supports the memory for novel related information. *Cerebral Cortex*, *27*, 1906–1921.
- Takashima, A., Nieuwenhuis, I. L., Rijpkema, M., Petersson, K. M., Jensen, O., & Fernandez, G. (2007). Memory trace stabilization leads to large-scale changes in the retrieval network: A functional MRI study on associative memory. *Learning & Memory*, *14*, 472–479.
- Tzourio-Mazoyer, N., Landeau, B., Papathanassiou, D., Crivello, F., Etard, O., Delcroix, N., ... Joliot, M. (2002). Automated anatomical labeling of activations in SPM using a macroscopic anatomical parcellation of the MNI MRI single-subject brain. *NeuroImage*, *15*, 273–289.
- Uncapher, M. R., & Rugg, M. D. (2009). Selecting for memory? The influence of selective attention on the mnemonic binding of contextual information. *The Journal of Neuroscience*, *29*, 8270–8279.
- Uncapher, M. R., & Wagner, A. D. (2009). Posterior parietal cortex and episodic encoding: Insights from fMRI subsequent memory effects and dual-attention theory. *Neurobiology of Learning and Memory*, *91*, 139–154.
- Utevsky, A. V., Smith, D. V., & Huettel, S. A. (2014). Precuneus is a functional core of the default-mode network. *The Journal of Neuroscience*, *34*, 932–940.
- van Buuren, M., Kroes, M. C., Wagner, I. C., Genzel, L., Morris, R. G., & Fernandez, G. (2014). Initial investigation of the effects of an experimentally learned schema on spatial associative memory in humans. *The Journal of Neuroscience*, *34*, 16662–16670.
- van den Broek, G. S., Takashima, A., Segers, E., Fernandez, G., & Verhoeven, L. (2013). Neural correlates of testing effects in vocabulary learning. *NeuroImage*, *78*, 94–102.
- van Kesteren, M. T., Ruiters, D. J., Fernandez, G., & Henson, R. N. (2012). How schema and novelty augment memory formation. *Trends in Neurosciences*, *35*, 211–219.
- Vilberg, K. L., & Rugg, M. D. (2008). Memory retrieval and the parietal cortex: A review of evidence from a dual-process perspective. *Neuropsychologia*, *46*, 1787–1799.
- Wagner, A. D., Shannon, B. J., Kahn, I., & Buckner, R. L. (2005). Parietal lobe contributions to episodic memory retrieval. *Trends in Cognitive Sciences*, *9*, 445–453.
- Wilms, M., Eickhoff, S. B., Homke, L., Rottschy, C., Kujovic, M., Amunts, K., & Fink, G. R. (2010). Comparison of functional and cytoarchitectonic maps of human visual areas V1, V2, V3d, V3v, and V4(v). *NeuroImage*, *49*, 1171–1179.
- Wing, E. A., Marsh, E. J., & Cabeza, R. (2013). Neural correlates of retrieval-based memory enhancement: An fMRI study of the testing effect. *Neuropsychologia*, *51*, 2360–2370.
- Woo, C. W., Krishnan, A., & Wager, T. D. (2014). Cluster-extent based thresholding in fMRI analyses: Pitfalls and recommendations. *NeuroImage*, *91*, 412–419.
- World Medical Association. (2013). World Medical Association Declaration of Helsinki: Ethical principles for medical research involving human subjects. *JAMA*, *310*, 2191–2194.
- Yarkoni, T. (2009). Big correlations in little studies: Inflated fMRI correlations reflect low statistical power—commentary on Vul et al. (2009). *Perspectives on Psychological Science*, *4*, 294–298.
- Zeithamova, D., Dominick, A. L., & Preston, A. R. (2012). Hippocampal and ventral medial prefrontal activation during retrieval-mediated learning supports novel inference. *Neuron*, *75*, 168–179.

SUPPORTING INFORMATION

Additional supporting information may be found online in the Supporting Information section at the end of the article.

How to cite this article: Schott BH, Wüstenberg T, Lücke E, et al. Gradual acquisition of visuospatial associative memory representations via the dorsal precuneus. *Hum Brain Mapp*. 2019;40:1554–1570. <https://doi.org/10.1002/hbm.24467>